Noise and Synchronization of a Single Active Colloid

Nicolas Bruot,[1] Loïc Damet,[1] Jurij Kotar,[1] Pietro Cicuta,[1] and Marco Cosentino Lagomarsino[2,3]
[1]*Cavendish Laboratory and Nanoscience Centre, University of Cambridge, Cambridge CB3 0HE, United Kingdom*
[2]*Genomic Physics Group, UMR 7238 CNRS "Microorganism Genomics," Paris, France*
[3]*University Pierre et Marie Curie, 15 rue de l'École de Médecine, Paris, France*
(Received 4 May 2011; published 24 August 2011)

A two-state oscillator in a viscous liquid is composed of a micron-scale particle whose intrinsic dynamics is defined by linear potentials that undergo configuration-coupled transitions and is externally driven by a piecewise constant periodic force of varying amplitude and frequency. This elementary example of "active matter" has the minimal elements that allow us to study synchronization in the presence of thermal fluctuations. Experiments reveal the presence of synchronized states (and Arnol'd tongues), which we explain using analytical and numerical calculations. The system maintains synchronization by adjusting the phase between the bead and the clock. We discuss the relevance of this model to synchronization in real-world systems, including the role of thermal noise.

DOI: 10.1103/PhysRevLett.107.094101 PACS numbers: 05.45.Xt, 05.40.Ca, 87.80.Cc

The coordinated motion of groups of two or more eukaryotic cilia or flagella is relevant for the role played in a wide range of biological systems, from propulsion of algae to fluid transport in the respiratory tract, or symmetry breaking in embryos [1]. Recent evidence from quantitative experiments supports the long-standing hypothesis [2] that hydrodynamic interactions are key in these synchronization phenomena [3]. For example, a recent study [4] found consistency between the synchronized behavior of the two flagella in the *Chlamydomonas* algae and a generic model of two coupled noisy phase oscillators with a coupling strength consistent with hydrodynamic interactions. However, the mechanochemical aspects of ciliary synchronization are still largely unknown.

Cilia synchronization involves both how the internal degrees of freedom are coupled to the external perturbations arising from the other active elements, and also the effects of thermal fluctuations. Thermal noise is relevant at the length scales and typical coupling forces involved [4,5]. Despite a few existing computational studies [4,6,7], the role of noise in these systems remains largely to be addressed, and is one of our focuses here.

In order to attack the problem of the internal drive, a number of minimal (deterministic) physical models with a reduced number of degrees of freedom have been developed [6–13]. These models fall into two main classes. The first class is based on rotating objects, with continuous close orbits. A second class of models [7,8,12] is not based on rotors, but rather the oscillator is a hydrodynamic bead that can be subject to two one-dimensional force potentials, which switch when a particular limit configuration is reached (a "geometric switch"). This system has the advantage of being experimentally feasible to study [7].

Here, in order to focus on the role of the geometric switch mechanics in synchronization, we further simplify the setting and address the response of a single two-state oscillator with linear potential to an external periodic force. This allows a deeper quantitative understanding of the synchronization properties and the role of noise in the experiment. Our results have relevance for the wider field of synchronizing systems, where few controlled experiments exist.

In the experiment, a time-shared optical laser trap creates a potential energy landscape which is linear in one direction. This allows us to apply a constant force F to an overdamped particle. In the absence of noise a bead of radius R would be driven at a constant velocity $v = F/\gamma$, with $\gamma = 6\pi\eta R$ and η the viscosity. The oscillation cycle is built from piecewise-constant slopes [Fig. 1(a)]. The main driving force F_d is applied to the particle. At the geometric boundary, this force is switched to its opposite, so that the particle is pushed the opposite way. The internal drive state is represented by a discrete variable $\sigma_d = \pm 1$. On top of this driven motion, in which the switch of potential is determined at the first-passage condition of the particle, we superpose an external "clock" signal, the period of which is set externally. The clock is realized itself as a time-variable tilt in the linear potential constructed by time-shared traps. It applies on the bead a weak force F_c that is also constant, and either strengthens or weakens the basic drive, depending on the clock state, which can be parameterized by a discrete variable $\sigma_c = \pm 1$. Therefore, at any time, the particle feels a force $\sigma_d F_d + \sigma_c F_c$, with the switches of σ_d and σ_c determined according to the geometric condition and the clock ticks. Experimentally, the total force is controlled by a computer that analyzes the position of the bead to get σ_d and uses its internal clock to get σ_c. Experiments were performed at room temperature (296 K) in water-glycerol solutions of viscosity 2.2×10^{-3} Pa · s, with spherical silica beads (Bangs Laboratories) of $R = 1.74 \pm 0.15$ μm.

 © 2011 American Physical Society

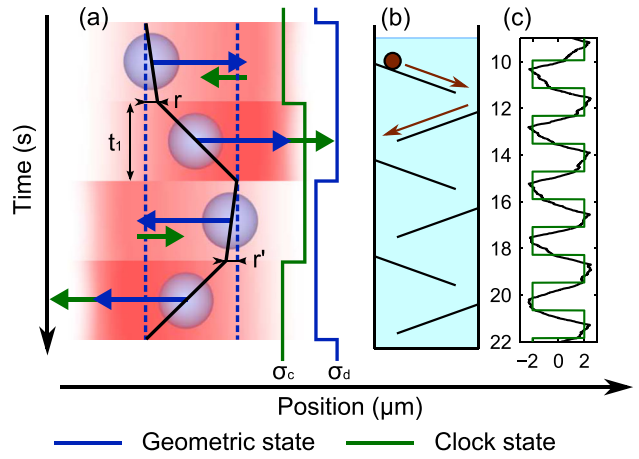

FIG. 1 (color online). A colloidal bead is driven with a combination of a fixed-period piecewise-constant force (the clock) and a linear potential with configuration-coupled switching. (a) Scheme of the experiment. The blue [dark gray] arrows represent the internal potential and the green [medium gray] arrows the clock. Both are realized with time-shared optical tweezers (red shades). Blue dashed lines are the switching positions. (b) Mechanical analogy with an overdamped ferromagnetic bead falling in an infinite set of slides and subject to a piecewise constant oscillating magnetic field gradient. (c) Oscillations from one experimental track (black). Experimental parameters are $a = 4.66\ \mu$m, $v = 3.91\ \mu\text{m} \cdot \text{s}^{-1}$, $\epsilon = 0.5$, $T_c = T_d = 2.38$ s.

The geometric switch condition, which sets the amplitude of oscillations to a, is analogous to a bead driven by gravity and falling through a system of tilted linear slides, in a high-viscosity fluid [Fig. 1(b)]. In this analogy, the external clock provides a modulating force in the right or left directions. The equation of motion is

$$\dot{x} = v[\sigma_d(t) + \epsilon\sigma_c(t)] + \zeta(t), \tag{1}$$

where $\epsilon v = F_c/\gamma$ and ζ is thermal (Gaussian, white) noise.

Let us consider first a clock with a period of $T_c = 2a/v$; thus, it is equal to the natural period of the oscillator T_d. The experimental trajectories of the colloidal particle position show synchronization with the clock state as a function of time [Fig. 1(c)]. The synchronized state is such that the configurational switches occur at midpoints between two clock switches. The existence of this synchronized state can be easily understood considering the system in absence of noise. Supposing we start from the position r immediately after a clock switch [Fig. 1(a)], and the clock is coherent with the internal state ($\sigma_c = \sigma_d = 1$). The time to the first geometric switch will be $t_1 = (a - r)/v(1 + \epsilon)$. Subsequently, $\sigma_d = -1$, and the clock will contrast the internal state for a time $t_2 = T_c/2 - t_1$, during which the bead will reach the position $r' = A + Br$, where $A = \kappa a\epsilon$, and $B = \kappa$, with $\kappa = (1 - \epsilon)/(1 + \epsilon)$. The remaining half of the cycle will follow an identical dynamics by

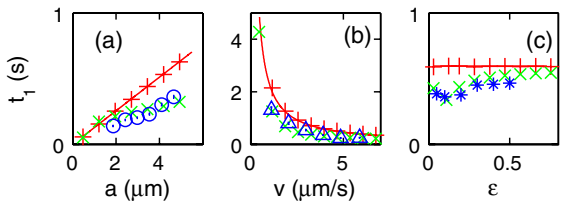

FIG. 2 (color online). Comparison of experiments, simulations, and theory for the mean delay t_1 between a geometric switch and a clock switch for $T_c = T_d$. Experiments (○, △ and *) and simulations including an adjustment for the bead size and delays in trap switches (×) agree and simulations without any correction (+) fit perfectly our theoretical formula for the fixed point (solid line). The dependence of t_1 with three parameters has been explored: (a) the amplitude a, (b) the mean velocity v and (c) the strength of the perturbation ϵ. The theoretical dependence corresponds to a constant phase equal to 1/4. While one parameter is varying, the others are fixed to the following values: $a = 4.66\ \mu$m, $v = 3.91\ \mu\text{m} \cdot \text{s}^{-1}$ and $\epsilon = 0.1$.

symmetry. The fixed point $r_{\text{fp}} = (1 - \epsilon)a/2$ follows immediately. This fixed point indicates the position where the particle will be found after a clock switch. It can be substituted to r in the above equations, to obtain the four time differences t_i between consecutive clock switches and geometric switches. These are equal to $T_c/4$. In other words, the system always puts itself at a phase difference $(\phi_1)_{\text{fp}} = (t_1)_{\text{fp}}/T_c$ of 1/4 between oscillator and clock.

The experimental results agree well with these predictions (Fig. 2). The small (5%–10%) deviations can be understood as by-products firstly of the finite image-analysis time and secondly of the uncertainty in the bead radius used in the experiment. First, the rate at which images are analyzed is not negligible (frame rate is 100 fps). Then, a further delay is added and represents the time between an image capture and the successive implementation of the trap position switch. In total, a feedback delay of 25 ms in the simulations fits with our experiments. Second, since calibration of the optical landscape is a lengthy process of refining the intensity of 62 traps, the experiments were of necessity performed on different beads, and there is a small variation in bead size between the experiment and the calibration, which we estimated by measuring its velocity. The correction is then included in the simulations as a modified Stokes drag. Both corrections have been included in our Ermak-McCammon algorithm simulations [7,14], giving excellent agreement with data of Fig. 2.

In the presence of thermal noise, each geometric switch time needs to be treated as a random variable, corresponding to the first-passage time between the previous clock switch and the geometric switch. This is a complex situation where uncertainties in subsequent switching times propagate between different subportions of a cycle. However a simple argument is sufficient to capture the

salient features of the fluctuations. Supposing that, for a half-cycle of index i, $t_1(i) = (t_1)_{\mathrm{fp}} + q(i)$, i.e., it is a sum of a deterministic value and some fluctuations, one obtains the effective equation $\delta q = q(i+1) - q(i) = -2q(i)\epsilon/(1+\epsilon) + \chi(i)$, where $\chi(i)$ is a random variable accounting for the effects of noise. χ can be estimated by summing two kinds of contributions. The first comes from the diffusion from the geometric switch point to the clock switch point, giving a variance $V_1 \simeq 2D(T_c/2 - \langle t_1 \rangle)/[v^2(1+\epsilon)^2]$, with D the diffusion coefficient. The second contribution comes from the trajectory between the clock switch and the subsequent geometric switch. It can be estimated as the difference between the first-passage time of a particle under drift $v(1+\epsilon)$ (with the initial condition corresponding to the mean position at the clock switch at distance x from the geometric switch) and the mean of the same first-passage time. This first-passage time is known to follow an inverse Gaussian distribution [15] which can be approximated by a Gaussian with variance $V_2 = 2xD/[v^3(1+\epsilon)^3] \simeq 2D\langle t_1 \rangle/[v^2(1+\epsilon)^2]$. In this case, the evolution of δq can be approximated as a simple continuous Langevin equation. Since over a half-cycle $\mathrm{var}(\chi) = V_1 + V_2$, the fluctuations for the switching time are estimated by $\langle q^2 \rangle = DT_c/[4\epsilon v^2(1+\epsilon)]$. A better estimate of the continuum limit for δq (presented in the Supplemental Material [16]) leads to the refined solution $\langle q^2 \rangle = DT_c/(4\epsilon v^2)$ or, equivalently, $\mathrm{std}(\phi_1) = \mathrm{std}(t_1/T_c) = \sqrt{\xi/(16\epsilon)}$, where std denotes the standard deviation and $\xi = 2D/(av)$ is a nondimensional measure of noise strength. This expression for the fluctuations around the synchronized state describes very well both experiments and simulations (Fig. 3).

Next, we analyze the consequences of a clock period that does not match the natural oscillation time of the oscillator, but is longer or shorter, $T_c = 2a/v + \delta$. Repeating the calculation sketched above, we see that the fixed point position r_{fp} is shifted by the quantity $(1-\epsilon^2)\,\delta v/(4\epsilon)$. In terms of switching times, this behavior is translated in the synchronized "phase difference"

$$\phi_1 = \frac{(t_1)_{\mathrm{fp}}}{T_c} = \frac{1}{4}\left(1 - \frac{(1-\tau)}{\epsilon}\right), \tag{2}$$

where $\tau = T_d/T_c$ measures the mismatch between oscillator and drive. This formula assumes that the sequence of geometric and clock switches is as shown in Fig. 1. It is therefore only valid for $\tau \in [1-\epsilon, 1+\epsilon]$. In other words, when changing the clock period, the system adapts its phase in the interval $[0, 1/2]$ in order to remain synchronized. When noise and detuning are present at the same time, the argument presented above can be repeated step-by-step with no further complications, leading to the expression

$$\mathrm{std}\,(\phi_1) = \sqrt{\xi\tau/(16\epsilon)}. \tag{3}$$

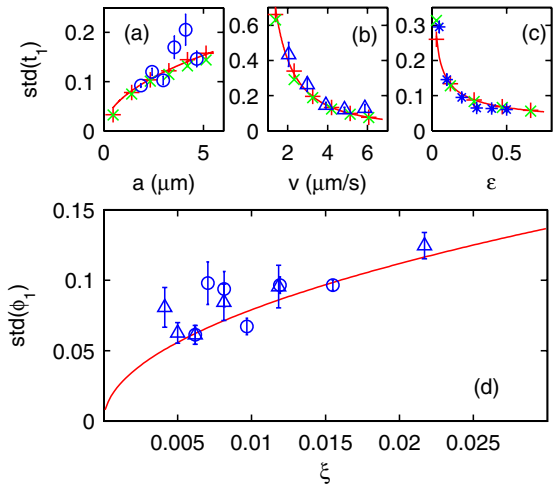

FIG. 3 (color online). Increasing noise ξ leads to higher fluctuations of the delay (phase) between a geometric switch and a clock switch. (a), (b), and (c) Theoretical predictions at 296 K (line) fit with both experiments (○, △, *) and simulations with (×) or without (+) experimental corrections. Parameters are the same as in Fig. 1. (d) As shown in our formula for the phase ϕ_1, represented by the solid line, the amplitude a and the mean velocity v can be merged in the strength parameter $\xi = 2D/(av)$. Error bars are the standard deviation of four different data sets.

Figure 4(a) presents experimental data showing phase slips emerging with detuning, and Fig. 4(b) explores numerically the dependence on τ of the phase difference accumulated in each cycle. The plateaus in Fig. 4(b) correspond to synchronized states [17], where the accumulated phase difference locks. The plateau at zero, around $\tau \simeq 1$, is the basic synchronized state and other

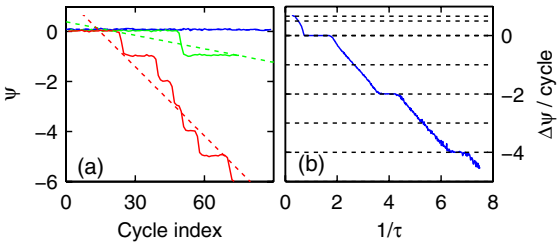

FIG. 4 (color online). Synchronization in the presence of mismatch in the natural frequencies of oscillator and clock. (a) shows how the experimental accumulated phase in time ψ depends on the detuning (solid lines). $1/\tau = 1.43$ (blue [dark gray]), 1.68 (green [light gray]) and 1.75 (red [medium gray]). For high detuning, phase slips occur determining phase difference accumulation. Dashed lines are linear fits, the gradient of which are the phase difference accumulated in each cycle. Extensive simulations in (b) show plateaus in the phase accumulation, at integer frequency ratios between oscillator and clock (integer ratios are highlighted by dashed lines). $T = 296$ K, $a = 4.66\ \mu$m, $v = 3.91\ \mu\mathrm{m}\cdot\mathrm{s}^{-1}$ and $\epsilon = 0.5$.

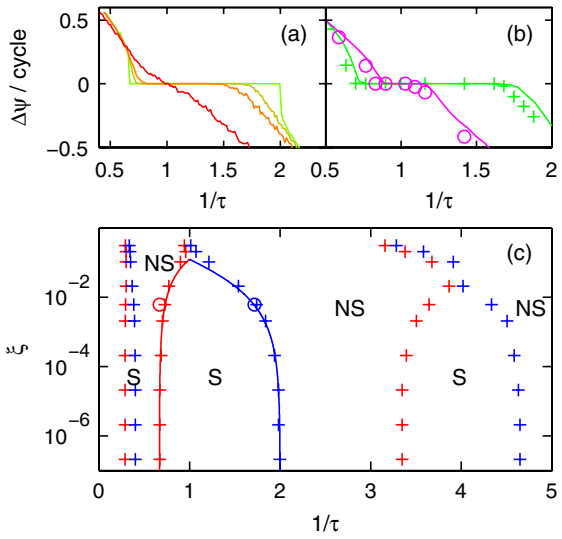

FIG. 5 (color online). The synchronization plateau width is affected by both noise level (a) (simulations with $\xi = 2.09 \times 10^{-7}$, 6.20×10^{-3}, 2.09×10^{-2}, 0.209 from green [light gray] to red [medium gray], and $\epsilon = 0.5$) and coupling strength ϵ (b) [simulations as lines, and experiments (○) at 296 K for perturbations $\epsilon = 0.2$ (magenta [medium gray]) and 0.5 (green [light gray])]. $a = 4.66$ μm and $v = 3.91$ $\mu\text{m} \cdot \text{s}^{-1}$. Note in (a) that for $T = 296$ K (i.e., $\xi = 6.20 \times 10^{-3}$), the synchronization is lost for $1/\tau \approx 1.7$, in agreement with Fig. 4(a). (c) Phase diagram representing the lower (red [medium gray]) and upper (blue [dark gray]) plateau boundaries depending on the noise $\xi = 2D/(av)$. Three plateaus are found in the $1/\tau \in [0.1, 5]$ range. Simulations (+), experiments (○), and theory (lines). The regions identify synchronized (S) and nonsynchronized states (NS).

synchronized states exist at particular integer ratios (identical to the Arnol'd tongues of nonlinear oscillators). The synchronization plateaus are affected by both noise level and detuning strength [Figs. 5(a) and 5(b)]. The results above can be collected as a phase diagram as a function of τ and the noise strength ξ, for a given modulation strength ϵ [Fig. 5(c)]. The values that delimit the synchronization region for the locked state with equal frequency can be estimated analytically using the expressions derived above for the fixed point of ϕ_1 and its variability. As a criterion for stability we have taken that the synchronization phase difference fixed point ϕ_1 should be placed at least 2 standard deviations away from the boundaries of 0 and $1/2$ set by the positions of the geometric switch [18]. This gives the thresholds observed in Fig. 5(c), in very good agreement with experiment and simulations.

In conclusion, the two-state geometric-switch oscillator analyzed here exhibits many features typical of a noisy nonlinear oscillator [17], similarly to rotatorlike models for cilia [9,10]. This is by itself remarkable, as the definition of its dynamics (with a discontinuous velocity) puts it *a priori* in a peculiar class of systems. As we have shown, its synchronization dynamics and the role of thermal noise as measured in experiments can be understood by simple quantitative arguments.

Considerations can be made on the noise threshold where synchronization is lost. At a given detuning level τ, this is set by the external perturbation ϵ and the variable $\xi = 2D/av \sim k_B T/W_{\text{stroke}}$, where $W_{\text{stroke}} = \gamma v a$ is the work performed by the rower on the fluid during one stroke. For synchronization to be observed, the ratio ξ/ϵ should not exceed a critical value of order 1. This sets a minimum scale for the size of the oscillator and its rowing amplitude. Plugging in realistic numbers [5], we estimate that the condition is always satisfied for flagella and cilia ($\xi \simeq 10^{-4}$ to 10^{-5}, $\epsilon \simeq 10^{-1}$). On the other hand, this might not always be the case for smaller systems. As an example, we estimate that ξ could be order 10^{-2} for stereocilia [19], which might put them near the critical limit. Indeed, it is observed that different bundles of stereocilia do not synchronize. While realistic situations are likely to involve more complex external drive and collective behavior, the simple system studied here highlights conditions and limits that are likely to apply to a range of systems including future artificial swimmers or synchronized micromotors.

We thank M. Polin and B. Bassetti for stimulating this work, J. Bechhoefer for critical review, and M. Baraldi for early contributions. Support from the Marie Curie ITN-COMPLOIDS (FP7-PEOPLE-ITN-2008 No. 234810).

[1] D. Bray, *Cell Movements: From Molecules to Motility* (Garland Science, New York, 2000).
[2] G. I. Taylor, Proc. R. Soc. A **209**, 447 (1951).
[3] R. Golestanian, J. Yeomans, and N. Uchida, Soft Matter **7**, 3074 (2011).
[4] R. E. Goldstein, M. Polin, and I. Tuval, Phys. Rev. Lett. **103**, 168103 (2009).
[5] M. Polin, I. Tuval, K. Drescher, J. P. Gollub, and R. E. Goldstein, Science **325**, 487 (2009).
[6] V. B. Putz and J. M. Yeomans, J. Stat. Phys. **137**, 1001 (2009).
[7] J. Kotar, M. Leoni, B. Bassetti, M. Cosentino Lagomarsino, and P. Cicuta, Proc. Natl. Acad. Sci. U.S.A. **107**, 7669 (2010).
[8] M. C. Lagomarsino, P. Jona, and B. Bassetti, Phys. Rev. E **68**, 021908 (2003).
[9] T. Niedermayer, B. Eckhardt, and P. Lenz, Chaos **18**, 037128 (2008).
[10] N. Uchida and R. Golestanian, Phys. Rev. Lett. **106**, 058104 (2011).
[11] M. Reichert and H. Stark, Phys. Rev. E **69**, 031407 (2004).
[12] C. Wollin and H. Stark, Eur. Phys. J. E **34**, 42 (2011).
[13] A. Vilfan and F. Jülicher, Phys. Rev. Lett. **96**, 058102 (2006).
[14] D. L. Ermak and J. A. McCammon, J. Chem. Phys. **69**, 1352 (1978).
[15] S. Redner, *A Guide to First-Passage Processes* (Cambridge University Press, Cambridge, England, 2001).

[16] See Supplemental Material at http://link.aps.org/supplemental/10.1103/PhysRevLett.107.094101 for details of the calculation that leads to an estimate of the fluctuations around the synchronized state.

[17] A. Pikovsky, M. Rosenblum, and J. Kurths, *Synchonization* (Cambridge University Press, Cambridge, England, 2001).

[18] In this condition the probability of phase slips is small, as there will be a slip every 43 cycles on average.

[19] J. Baumgart, M. Fleischer, Y. M. Yarin, and R. Grundmann, in *8th International Symposium on Experimental and Computational Aerothermodynamics of Internal Flows, Lyon (France)*, edited by X. Ottavy and I. Trebinjac (2007), Vol. 1, pp. 189–193.